Available online at www.sciencedirect.com
ScienceDirect
Electrochimica Acta 53 (2007) 644–649
ELECTROCHIMICA Acta
www.elsevier.com/locate/electacta

Effect of temperature on Co electrodeposition in the presence of boric acid

J.S. Santos, R. Matos, F. Trivinho-Strixino, E.C. Pereira *

NANOFAEL, CMDMC, Departamento de Química, Universidade Federal de São Carlos, Cx 676, São Carlos, SP, Brazil

Received 25 April 2007; received in revised form 11 July 2007; accepted 12 July 2007
Available online 19 July 2007

Abstract

The electrodeposition of cobalt from sulphate solutions containing boric acid was investigated using EQCM technique coupled with potentiostatic measurements. The boric acid was added to electrolyte as a buffer to avoid the local pH rise caused by parallel hydrogen evolution reaction (HER). The results showed that the buffer contribution of boric acid is effective in the cobalt electrodeposition at 25 °C; however, cobalt hydroxide is formed simultaneously with cobalt deposition at 48 °C. The *M*/*z* values calculated using the Sauerbrey equation and the Faraday Law showed that in the initial stages of deposition at 48 °C, only cobalt deposits were detected, but after 2 s, an important amount of $Co(OH)_2$ started to be formed.

Keywords: Cobalt; Cobalt hydroxide; Electrodeposition; Morphology; EQCM

1. Introduction

While the recent advances in the nanomaterial science have opened up new possibilities for the fabrication of new devices, they have also raised new issues. As an example, a number of these involve the problems that arise in dealing with the electrodeposition of metals with magnetic properties over substrates with specific pattern for the storage devices industry [1–3]. Furthermore, the structure and morphology control is an essential task in the electrodeposition of metals with magnetic property. This property, as well others such as hardness, thermal stability and corrosion resistance of cobalt electrodeposits has motivated further investigations on cobalt electrodeposition [4–6]. Depending on the preparation conditions, *i.e.* electrolyte composition, pH of the solution, temperature, current density and the presence of additives, different morphological and structure properties can be obtained [6–10]. As these problems are not addressed at all in this field, the study of the cobalt electrodeposition mechanism is of particular interest.

During the metal electrodeposition in aqueous solution parallel processes can occur. An important secondary process is the parallel hydrogen evolution reaction (HER), which may strongly affect the morphological and structural properties and decrease the overall process efficiency [11–14]. According to some authors [11,13], the pH near the electrode surface could increase due to the water electrolysis leading to hydroxide ions formation and hydrogen evolution reaction, as follows:

$$H_2O + M\text{–}H + e^- \rightarrow M + H_2(ads) + OH^- \quad (a)$$

From reaction (a), one can observe that the adsorption mechanism is an important task to be considering in electrodeposits carried out simultaneously with HER [8,11–14]. Hence, the hydrogen electrodic desorption rate (V_{ed}) must be considered for the investigation of the overall mechanism during electrodeposition process and their parameters dependence (*i.e.*, temperature, the surface fraction covered with adsorbed hydrogen (θ) and the pH in the double layer region). In this subject, some authors [9,15] suggested that the temperature may affect the HER raising its rate. Thus, for high temperatures, the electrodeposition process efficiency could drop down to 60% and the hydrogen adsorption process would become less favorable modifying the hydrogen electrodic desorption rate (V_{ed}).

On the other hand, to avoid the pH variation near the electrode, it is also common to add boric acid (H_3BO_3) in the electrolyte to inhibit the formation of hydroxide species [10,16–20]. Unfortunately, the real function of this additive in electrodeposition is yet a matter of controversy and a lot of

* Corresponding author. Tel.: +55 16 33518214/213; fax: +55 16 33518214.
E-mail address: decp@power.ufscar.br (E.C. Pereira).

0013-4686/$ – see front matter © 2007 Elsevier Ltd. All rights reserved.
doi:10.1016/j.electacta.2007.07.025

propositions were done. Most authors proposed that the boric acid acts mainly as a buffer agent [16–18]. This effect is thought to be a dynamic process occurring during the HER. Consequently, the dissociation kinetics of the buffer must be fast enough to supply protons during molecules discharge occurring at the electrode surface. Studying this behavior, Horkans [19] concluded that the dissociation of HSO_4^- as well as H_3BO_3 is so slow that the overall buffer contribution is ineffective during HER in sulphate electrolyte. However, this author also proposed that this additive may act as a homogeneous catalyst which decreases the metal electrodeposition overpotential [19]. In addition, Yin and Lin [20] proposed that H_3BO_3 works as a selective membrane inhibiting movement of the ions during diffusion controlled process at the electrode.

Considering how these parameters (temperature, the surface fraction covered with adsorbed hydrogen (θ) and the pH in the double layer region) could affect the electrodeposition process, much effort has been given to elucidate the mechanism of cobalt electrodeposition. The main idea lies on the assumption that the pH in the vicinity of the cathode surface increases due to hydrogen evolution and cobalt hydroxide can be formed. From this point of view, numerous authors proposed different and/or complementary mechanism for cobalt electrodeposition. According to Jiang and Tseung [21], Co deposition occurs through the reduction of a cobalt complex, such as $CoOH^+$, and the limiting step was the reduction of CoOH to metallic Co. In another paper, Pradhan et al. [14] also suggested that the cobalt electrodeposition mechanism occurs via formation of $CoOH^+$ at more acidic pH values. The propositions of these authors [14] consider that there is a surface fraction covered by adsorbed hydrogen and the reaction proceeds through $CoOH^+$ and H_{ads} reduction. However, rising the pH (at pH 4 and 4.5) the mechanism involves $Co(OH)_2$ formation. On the other hand, we described elsewhere [22] that cobalt hydroxide is formed simultaneously with Co deposition during the early stages of reduction at pH 4.10 under borate free electrolytes. However, at pH 3.33 only the direct cobalt reduction is observed without any hydroxide species formation.

Although significant advances have been made in the understanding of how additives and temperature influence the cobalt electrodeposition, very little attention appears to have been given to the exact role of these parameters on the electrodeposition process. Hence, the objective of the present study is to investigate the cobalt electrodeposition using the electrochemical quartz crystal microbalance (EQCM) in the presence of H_3BO_3 at two different temperatures (25 °C and 48 °C).

2. Materials and methods

The experiments were carried out in a glass cell. The working electrode (WE) was a 9 MHz AT-cut quartz crystal coated with a Pt film in contact with the electrolyte ($A = 0.2\,cm^2$). The sensitivity of the EQCM used was 858.8 Hz μg^{-1}. The counter electrode (CE) was a Pt sheet and all potentials are referred to saturated calomel electrode (SCE). The resonance frequency shift was measured with a Seiko EG&G quartz crystal microbalance (model QCA 917). The electrochemical measurements were conducted using an EG&G PAR 263 A potentiostat/galvanostat.

All potentiodynamic and potentiostatic reactions were carried out at two temperatures (25 °C and 48 °C) using 0.05 mol L^{-1} $CoSO_4{\cdot}5H_2O$ + 0.01 mol L^{-1} H_3BO_3 + 0.113 mol L^{-1} Na_2SO_4 as supporting electrolyte (pH 5.0 at $T = 25$ °C). The electrochemical cell was maintained at a constant temperature using a thermostatic bath. The working electrode was cleaned using fast sweeping rate technique under 0.1 mol L^{-1} H_2SO_4 solution between −0.25 V and 1.20 V (versus SCE) until a satisfactory response of the Pt profile was obtained. All solutions were prepared with deionized water and analytical grade reagents. Before each experiment, the supporting electrolyte solution was bubbled with N_2 flux during 25 min.

3. EQCM data processing

The EQCM technique combined with cyclic voltammetry is a convenient tool to investigate electrochemical reactions by measuring the current, charge and related mass changes at the working electrode [23]. According to the Sauerbrey equation [24] the frequency variation (Δf) of the quartz crystal is correlated with the mass change on the electrode (Δm), as follows:

$$\Delta f = \frac{-2 f_0^2 \Delta m}{A\sqrt{\mu_i \rho_i}} = -K\Delta m \tag{1}$$

where f_0 is the resonant frequency of the quartz crystal, A the piezoelectric active area, μ_i the shear modulus of the quartz, K the experimental mass coefficient and ρ_i is the density of quartz. When Eq. (1) is combined with the Faraday Law, and the number of electrons involved in the reaction is known, the apparent molar mass can be calculated [24–26]. Hence, M/z values can be determined by fitting the slope of the mass versus charge curves:

$$\frac{M}{z} = \left|\frac{d\Delta f}{dQ}\right| \left(\frac{F}{K}\right) \tag{2}$$

where M is the molar mass of the deposit, F the Faraday constant and z is the number of electrons. The M/z values may also be used to evaluate the number of reactions occurring during an electrochemical process.

In the present paper, the M/z values were determined from potentiodynamic and potentiostatic measurements in $CoSO_4$ solution containing boric acid as a buffer at two temperatures (25 °C and 48 °C).

4. Results

A preliminary investigation to evaluate the main processes during the cobalt electrodeposition was performed using triangular voltammetry. Fig. 1 shows the voltammograms for the cobalt electrodeposition performed at two different temperatures and the corresponding mass change observed during the process. In the scan toward negative potentials there is no process until the beginning of cobalt deposition at −0.76 V (25 °C). For potentials more negative than this, an increase in the current and a mass change on the working electrode were observed (Fig. 1C). The cobalt reduction current peak is observed at −1.04 V (25 °C) followed by a significant increase in the cathodic current which

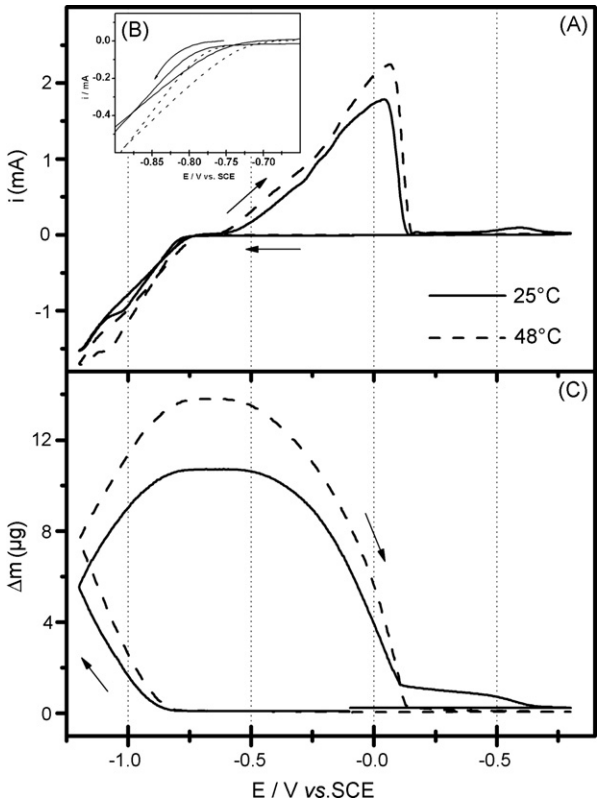

Fig. 1. (A) Cyclic voltammograms, (B) detailed range of cobalt deposition overpotential and (C) mass change as a function of potential in solution containing 0.05 M $CoSO_4$ + 0.01 M H_3BO_3 + 0.113 M Na_2SO_4 at pH 5.0 for cobalt electrodeposition at 25 °C and 48 °C. Scan rate = 20 mV/s.

can be associated with proton reduction. In the reverse sweep toward positive potentials, two crossing over potentials were observed. Furthermore, from Fig. 1A, one can observe an intense anodic peak with a shoulder during the cobalt dissolution which was previously reported by other authors [12,15,22,27,28]. This shoulder could be related to the dissolution of hydrogen rich cobalt phase [28]. The possibility of passivation should not be disregarded as cobalt(III) species could be formed, such as CoOOH, originated from the oxidation of $Co(OH)_{ads}$ or $Co(OH)_2$ previously adsorbed on the electrode. However, at any rate, all deposited material was dissolved during the anodic stripping (Fig. 1C).

Although the general profile of these two voltammograms (Fig. 1) has the same behavior for both temperatures, some important issues can be pointed out: (i) the overpotential of the cobalt deposition in the experiment carried out at 48 °C is smaller than the one at 25 °C (inset Fig. 1B), (ii) the mass–potential curves showed an increase in the deposited mass over the working electrode for the measurement performed at 48 °C, (iii) the total deposited mass on the electrode is dissolved (Fig. 1C) and (iv) the dissolution current peak related to the rich hydrogen phase is more evident in the electrodeposition carried out at 48 °C.

In our previous work [22], we showed that during the initial stages of cobalt electrodeposition, small quantities of $Co(OH)_2$ are produced. In the present work, we introduced the boric acid and changed the electrolyte temperature. In order to evaluate the species participating during the cobalt electrodeposition, the apparent *M*/*z* values (Tables 1 and 2) were calculated using the Faraday Law. Considering an ideal cobalt reduction involving 2 mol of electrons, the apparent *M*/*z* value must be 29.5 g mol^{-1} (MW Co = 58.9 g mol^{-1}). Following:

$$Co^{2+}(aq) + 2e^- \rightarrow Co(s) \quad (b)$$

The $Co(OH)_2$ formation requires an apparent *M*/*z* value of 46.5 g mol^{-1} (MW $Co(OH)_2/2e^-$) following the global reaction from (c) and (d):

$$2H_2O + 2e^- \rightarrow H_2(g) + 2OH^-(aq) \quad (c)$$

$$Co^{2+}(aq) + 2OH^-(aq) \rightarrow Co(OH)_2(ads) \quad (d)$$

Table 1 illustrates the apparent *M*/*z* value for potentiodynamic cobalt electrodeposition toward more negative potentials (from −0.8 V to −1.2 V), calculated using the slope of mass × charge curves and the Faraday Law (Fig. 2A). It was observed that for the experiment performed at 25 °C, there is only one apparent *M*/*z* in the whole potential window (31 ± 0.5 g mol^{-1}). This result shows that the electrodeposition follows the reaction (b), *i.e.* direct cobalt reduction. Different apparent *M*/*z* values were calculated for the experiment performed at 48 °C, as it can be observed in the slope variation during the potentiodynamic deposition depicted in Fig. 2B. Just at the beginning of cobalt reduction (from −0.86 V to −1.01 V) the *M*/*z* value was 38 ± 0.5 g mol^{-1}, which has an important component related to the global reaction originated from (c) and (d), where $Co(OH)_2$ is formed. In the subsequent process, the calculated *M*/*z* values were 32 ± 0.5 g mol^{-1} (from −1.01 V to −1.17 V) and 28 ± 0.5 g mol^{-1} (from −1.17 V to −1.20 V) indicating only cobalt reduction. The $Co(OH)_2$ could be reduced to Co at potential more negative than −0.97 V (Standard Potential [29,30]), following the reaction below:

$$Co(OH)_2(ads) + 2e^- \rightarrow Co(s) + 2OH^-(aq) \quad (e)$$

Table 1
Apparent *M*/*z* values calculated from Fig. 1A considering the total mass (Δ*m*) and charge (Δ*Q*) during cobalt electrodeposition toward negative potentials

Temperature (°C)	Potential range (V)	*M*/*z* (g mol^{-1})
25	−0.80 → −1.20	31 ± 0.5
48	−0.86 → −1.01	38 ± 0.5
	−1.01 → −1.17	32 ± 0.5
	−1.17 → −1.20	28 ± 0.5

Table 2
Apparent *M*/*z* values calculated considering the total mass (Δ*m*) and charge (Δ*Q*) from current–time transient experiment

Temperature (°C)	*M*/*z* (g mol^{-1})	
	Time: 0–2 s	Time: 2–10 s
25	27 ± 0.5	30 ± 0.5
48	30 ± 0.5	44 ± 0.5
25[a]	30 ± 0.5	31 ± 0.5

[a] After cooling procedure.

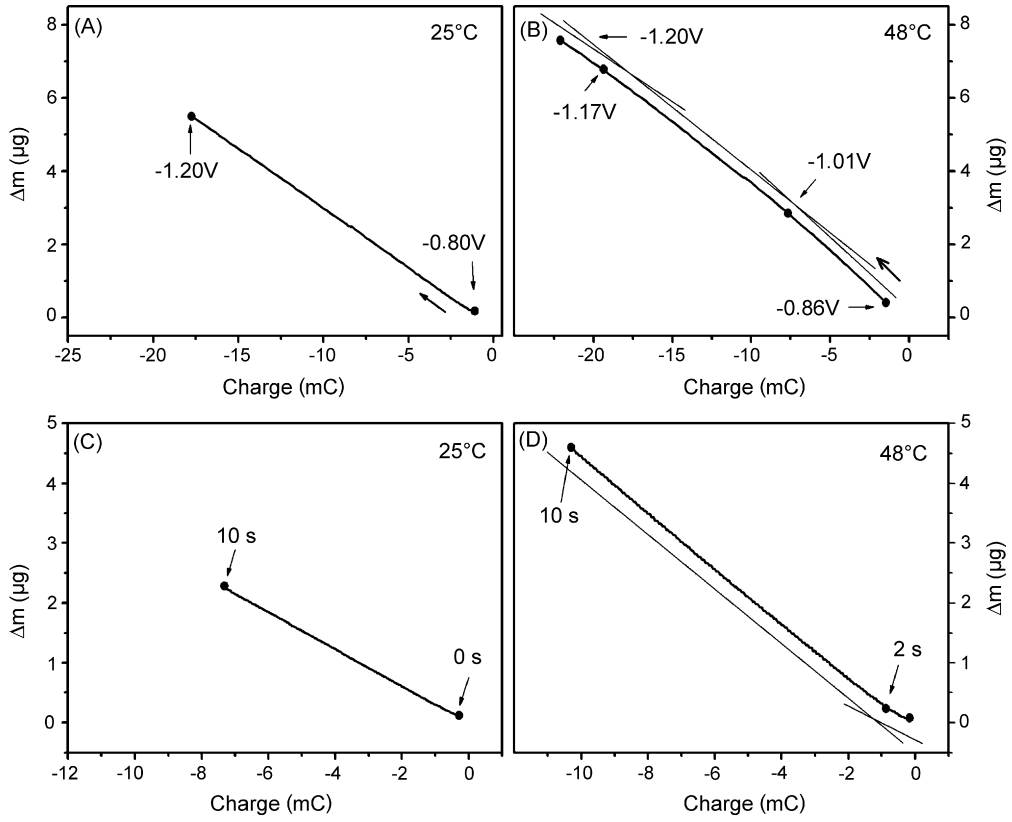

Fig. 2. Mass variation as a function of charge for (A and B) potentiodynamic deposition and (C and D) potentiostatic deposition at −095 V.

Hence, the $Co(OH)_2$ reduction requires an apparent M/z value of 23.2 g mol^{-1} ($M_{Co(OH)_2}/4e^-$) following reactions (c)–(e). If this is correct, one needs to consider 4 mol of electrons during all process. An apparent M/z value smaller than 29.5 g mol^{-1} shows that a mixed contribution from reactions (b) and (e) may also occur for the deposition performed at potentials more negative than −0.97 V (Standard Potential).

To study the electrodeposition process in a more detailed way, transient measurements coupled with EQCM were performed and the results are presented in Fig. 3 and Table 2. In these experiments, a step potential was applied between −0.1 V (where no faradaic reaction occurs on the electrode) and −0.95 V for 10 s. The chosen potential is located near the water electrolysis potential, where the HER occurs, and remains more positive than −0.97 V, which is the Standard Potential for $Co(OH)_2$ reduction [29,30]. It is important to stress that in these experimental condition the major fraction of produced $Co(OH)_2$ will not be reduced to Co. After the potentiostatic deposition, anodic stripping was performed to investigate the dissolution process and to evaluate the current efficiency.

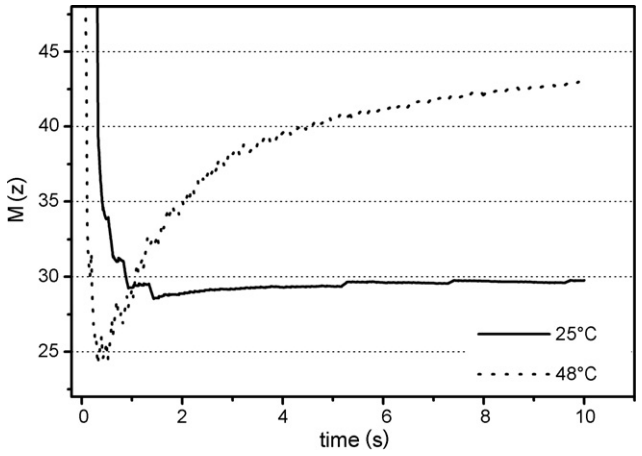

Fig. 3. Apparent M/z transients as a function of time.

Table 2 illustrates the M/z values calculated by fitting the slope of mass versus charge (Fig. 2C and D) for cobalt deposition at −0.95 V. During the cobalt deposition carried out at 25 °C, the calculated M/z value was 27 ± 0.5 g mol^{-1} (up to 2 s) and 30 ± 0.5 in the subsequent deposition (Fig. 2C). These values are very close to the theoretical value for cobalt reduction, indicating that the major reaction occurring on the electrode is described by reaction (b). In this case, it is not expected that the $Co(OH)_2$ reduction takes place since it was not produced at this experimental condition.

On the other hand, for the electrodeposition performed at 48 °C, at the first 2 s, the calculated M/z value was 30 ± 0.5 g mol^{-1} (Fig. 2D). Again, this suggests that in the initial stages of cobalt reduction the process proceeds through reaction (b). Within the interval between 2 s and 10 s, the calculated M/z value was 44 ± 0.5 g mol^{-1}. This value is in accordance with the global reaction originated from (c) and (d), which are related to $Co(OH)_2$ formation. The same result can be better visualized in Fig. 3, where the calculated apparent M/z transient

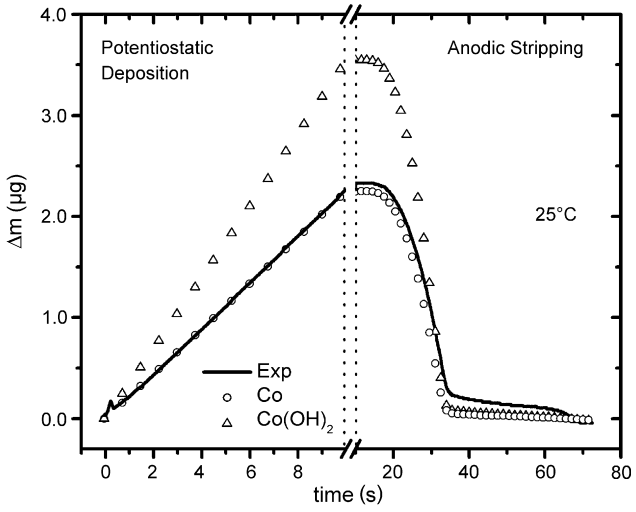

Fig. 4. Comparison of experimental and theoretical mass change of cobalt deposition and anodic stripping obtained at −0.95 V from current–time transients. $T = 25\,^{\circ}C$. Scan rate: 20 mV/s.

showed a continuous variation of the M/z values as a function of time. For the electrodeposition performed at 25 °C, the apparent M/z transient remains constant during all experiment indicating an electrodeposition mechanism where only cobalt is reduced. In addition, for the experiment carried out at 48 °C, one can observe a smooth increase of the apparent M/z transient, indicating a change in the cobalt electrodeposition mechanism starting with cobalt deposition followed by $Co(OH)_2$ formation occurring simultaneously with cobalt deposition up to 10 s. Although it was not expected, the sharp decrease of the M/z value at the early stage of the deposition process (0–0.5 s) could be related to reactions (c)–(e), which are related to the $Co(OH)_2$ reduction. However, the large experimental error due to the slow acquisition rate of the EQCM data may also be responsible for this sharp decrease in the beginning of the reduction process.

Figs. 4 and 5 illustrate the theoretical and experimental mass change over the working electrode during potentiostatic deposition and anodic stripping process for 25 °C and 48 °C, respectively. Fig. 4 depicts the theoretical mass variation for Co and $Co(OH)_2$ calculated considering the Faraday Law for reactions (b) and (d), respectively. For the experiment performed at 25 °C, the experimental mass change and the Co theoretical one overlapped during the potentiostatic deposition and the anodic stripping, which indicates that the electrodeposition occurs only via reaction (b). Hence, the current efficiency during this process is almost 100%. On the other hand, from the experiment performed at 48 °C (Fig. 5), one can observe that the experimental and Co theoretical curves overlapped up to 2 s, suggesting an electrodeposition mechanism via reaction (b). For times longer than this, the experimental curve drifts apart from the Co theoretical one and approaches the $Co(OH)_2$, indicating an electrodeposition process occurring via reaction (d), *i.e.* $Co(OH)_2$ formation. This behavior can also be observed during the anodic stripping and can be related to a decrease in the current efficiency. These data also confirmed the apparent calculated M/z values (Table 2) found by electrodeposition (−0.95 V) and dissolution at 48 °C suggesting that the electrodeposition mechanism is followed by a mixed contribution of different intermediary reactions, *i.e.* following reactions (b)–(d). After that, from the difference between the curves presented in Fig. 5, it was estimated that, at 10 s, almost 80% of the deposited material could be $Co(OH)_2$.

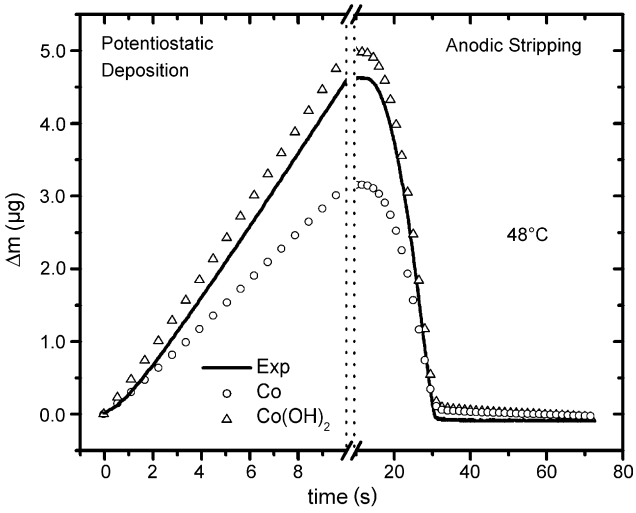

Fig. 5. Comparison of experimental and theoretical mass change of cobalt deposition and anodic stripping obtained at −0.95 V from current–time transients. $T = 48\,^{\circ}C$. Scan rate: 20 mV/s.

5. Discussion

The apparent M/z values related to hydroxide species were not expected in our experiments as H_3BO_3 was used to prevent any important pH variation near electrode surface. However, the real function of the boric acid during electrodeposition process is yet a matter of controversy, as initially stated in the introductory section. Despite all mechanism propositions, the data showed that the boric acid was ineffective for the experiment performed at 48 °C. Several propositions can be pointed out in order to explain our experimental data. First of all, an important experiment was performed to ensure that the boric acid did not lose its effectiveness during the experiments at high temperatures. For this purpose, subsequent electrodeposition was performed immediately after the experiment at 48 °C, cooling the solution until 25 °C. In this last measurement, at 25 °C, the cobalt was deposited at −0.95 V for 10 s and the apparent M/z value was calculated. Table 2 shows that the apparent M/z values after the cooling procedure was close to 30 g mol^{-1} (cobalt reduction via reaction (b)). These data revealed that the boric acid remains effective after the experiment performed at 48 °C, in which the additive was ineffective. Hence, any proposition about the deactivation of H_3BO_3 could be disregarded.

Jeffrey et al. [9] and Elsherief [15] proposed in their work that the HER contribution is intense in experiments carried out at high temperatures. If we consider that the hydrogen evolution reaction is more effective at 48 °C, the formation rate of OH^- ions must be larger than in the case of the experiment carried out at 25 °C. This explains the observed M/z values for hydroxilate species (Tables 1 and 2). Another effect of the temperature that is observed is a drift toward more positive overpotential for

the cobalt and proton reduction (Fig. 1B). However, the most suitable explanation for the inefficiency of boric acid may arise from the propositions described in the literature [10,17–19].

One possible mechanism involving complex ions formation can also be evoked, as the one proposed by Hoare [17]. This author proposed that H_3BO_3 can form a stable complex with the Ni ions making easier the discharge of this metal over the electrode. This author also suggests that the boric acid behaves like a homogeneous catalyst decreasing the overpotential for Ni deposition. Unfortunately, the mechanism for this proposition cannot be determined from our experimental results and more effort must be taken in order to consider this mechanism.

However, within the scope of our experimental result, we proposed that there is a mixed contribution of the slow dissociation kinetics of the boric acid and a mechanism involving adsorption of neutral boric acid molecules over the electrode, as proposed by Horkans [19]. This author proposed that in Ni deposition under SO_4^{2-} solution, little competition between H_3BO_3 and sulphates ions exists, and consequently, boric acid adsorption may decrease the active surface area. A local increase of the temperature in the electrode surface may strongly affect the adsorption rate of this species and change the cobalt deposition efficiency. As a result, the proton reduction rate will increase favoring the formation of hydroxilate species due to OH^- formation. On the other hand, if we consider the kinetics of the boric acid dissociation [19], it can be proposed that this dissociation is the rate-determining step during HER. In this case, the dissociation rate is not fast enough to provide the increase of concentration of OH^- at the surface of the electrode for the experiments performed at 48 °C. Although both hypotheses corroborate our experimental results, we propose that the contribution of the first proposition is more important to explain our experimental results than the one about the dissociation kinetics of boric acid, since it was observed that at 48 °C, the hydrogen evolution is intense. Besides, in the present case, the concentration of boric acid is lower (compared to the cobalt sulphate) than those investigations described in the literature for Ni deposition [17,19,31].

6. Conclusions

The analysis of the EQCM data and the current–time transient measurements indicated that the mechanism of cobalt electrodeposition changed when the temperature was increased in sulphate solution containing boric acid. At 25 °C, only direct cobalt reduction is observed, while in electrodeposition at 48 °C, $Co(OH)_2$ can be observed from the calculated apparent M/z values. These results suggest that $Co(OH)_2$ can be formed simultaneously with Co deposits and the buffer contribution of boric acid was ineffective at 48 °C. Furthermore, some propositions were considered to explain the inefficiency of the boric acid. The most suitable alternative is the one concerning the effect of temperature rise on the adsorption mechanism of H_3BO_3 over the electrode. For high temperatures, the desorption mechanism is greater, leading to an increase of the active surface area available for HER and, as a result, $Co(OH)_2$ can be formed.

Acknowledgments

The authors are grateful to FAPESP and CNPq for the financial support.

References

[1] S. Armyanov, Electrochim. Acta 45 (2000) 3323.
[2] P.L. Cavallotti, A. Vicenzo, M. Bestetti, S. Franz, Surf. Coat. Technol. 169–170 (2003) 76.
[3] M.V. Rastei, S. Colis, R. Meckenstock, O. Ersen, J.P. Bucher, Surf. Sci. 600 (2006) 2178.
[4] E. Gómez, E. Vallés, J. Appl. Electrochem. 32 (2002) 693.
[5] J. Dille, J. Charlier, R. Winand, J. Mater. Sci. 32 (1997) 2637.
[6] A. Azizi, A. Sahari, M.L. Felloussia, G. Schmerber, C. Miny, A. Dinia, Appl. Surf. Sci. 228 (2004) 320.
[7] C.Q. Cui, S.P. Jiang, C.C. Tseung, J. Electrochem. Soc. 137 (1990) 3418.
[8] S. Nakahara, S. Mahajan, J. Electrochem. Soc. 127 (1980) 283.
[9] M.I. Jeffrey, W.L. Choo, P.L. Breuer, Miner. Eng. 13 (2000) 1231.
[10] B.C. Tripathy, P. Singh, D.M. Muir, Metall. Trans. B 32 (2001) 395.
[11] D.R. Gabe, J. Appl. Electrochem. 27 (1997) 908.
[12] M. Palomar-Pardavé, B.R. Scharifker, E.M. Arce, M. Romero-Romo, Electrochim. Acta 50 (2005) 4736.
[13] M. Rojas, C.L. Fan, H.J. Miao, D.L. Piron, J. Appl. Electrochem. 22 (1992) 1135.
[14] N. Pradhan, T. Subbaiah, S.C. Das, U.N. Dash, J. Appl. Electrochem. 27 (1997) 713.
[15] A.E. Elsherief, J. Appl. Electrochem. 33 (2003) 43.
[16] N. Zech, D. Landolt, Electrochim. Acta 45 (2000) 3461.
[17] J.P. Hoare, J. Electrochem. Soc. 133 (1986) 2491.
[18] B.V. Tilak, A.S. Gendron, M.A. Mosoiu, J. Appl. Electrochem. 7 (1977) 495.
[19] J. Horkans, J. Electrochem. Soc. 126 (1979) 1861.
[20] K.M. Yin, B.T. Lin, Surf. Coat. Technol. 78 (1996) 205.
[21] S.P. Jiang, A.C.C. Tseung, J. Electrochem. Soc. 137 (1990) 3387.
[22] J.T. Matsushima, F. Trivinho-Strixino, E.C. Pereira, Electrochim. Acta 51 (2006) 1960.
[23] D.A. Buttry, in: H.D. ABRUNÃ (Ed.), The Quartz Crystal Microbalance as an In Situ Tool in Electrochemistry, 1, VHC, New York, 1991, p. 10.
[24] H.A.K.M. Saloniemi, M. Ritala, M. Leskela, J. Electroanal. Chem. 482 (2000) 139.
[25] J.G.N. Matias, J.F. Julião, D.M. Soares, A. Gorenstein, J. Electroanal. Chem. 431 (1997) 163.
[26] A. Marlot, J. Vedel, J. Electrochem. Soc. 1 (1999) 177.
[27] A.B. Soto, E.M. Arce, M. Palomar-Pardavi, I. Gonzalez, Electrochim. Acta 41 (1996) 2647.
[28] S. Jaya, T. Prasada Rao, G. Prabhakara Rao, Electrochim. Acta 32 (1987) 1073.
[29] S.P. Jiang, Y.Z. Chen, J.K. You, T.X. Chen, A.C.C. Tseung, J. Electrochem. Soc. 137 (1990) 3374.
[30] D.R. Lide, CRC Handbook of Chemistry and Physics, CRC Press, Florida, 1992, pp. 8–26.
[31] J. Horkans, J. Electrochem. Soc. 128 (1981) 45.